

Available online at [www.sciencedirect.com](http://www.sciencedirect.com)

ScienceDirect

journal homepage: [www.e-jds.com](http://www.e-jds.com)

Original Article

# Biocompatibility and pro-mineralization effect of tristrontium aluminate cement for endodontic use

Sherif Adel <sup>a,b</sup>, Kentaro Hashimoto <sup>a\*</sup>, Nobuyuki Kawashima <sup>a</sup>,  
Takahiro Wada <sup>c</sup>, Motohiro Uo <sup>c</sup>, Takashi Okiji <sup>a</sup>

<sup>a</sup> Department of Pulp Biology and Endodontics, Graduate School of Medical and Dental Sciences, Tokyo Medical and Dental University (TMDU), Tokyo, Japan

<sup>b</sup> Department of Restorative and Dental Materials, Oral and Dental Research Division, National Research Centre of Egypt, Cairo, Egypt

<sup>c</sup> Department of Advanced Biomaterials, Graduate School of Medical and Dental Sciences, Tokyo Medical and Dental University (TMDU), Tokyo, Japan

Received 2 December 2021; Final revision received 25 December 2021

Available online 6 January 2022

## KEYWORDS

Strontium aluminate;  
Endodontic cement;  
Cell proliferation;  
Cell attachment;  
Odonto/osteogenic  
differentiation;  
Mineralization

**Abstract** *Background/purpose:* Tristrontium aluminate ( $S_3A$ ) is a hydraulic cement with setting behavior similar to that of mineral trioxide aggregate (MTA). This study examined the biological effects of  $S_3A$  on mouse dental papilla cells (MDPs) *in vitro* and on rat exposed pulps *in vivo*.

*Materials and methods:* Extracts of  $S_3A$  and MTA were prepared by immersing each cement in ultrapure water. MDPs were cultured with  $S_3A$  or MTA extracts, and cell proliferation was evaluated with a tetrazolium-salt assay. Attachment of MDPs on the set cements was examined with scanning electron microscopy (SEM). mRNA expression of bone morphogenic protein (Bmp2), osteocalcin (Oc) and osteopontin (Opn) in MDPs exposed to  $S_3A$  or MTA extracts was determined with reverse transcription-quantitative polymerase chain reaction. Mineralized nodule formation was evaluated with Alizarin Red S staining. Simulated body fluid (SBF)-dipped  $S_3A$  was examined with SEM and energy dispersive X-ray analysis (EDX). Exposed molar pulps of male Wistar rats capped with  $S_3A$  or MTA were histologically examined.

*Results:*  $S_3A$  extract did not inhibit proliferation of MDPs. Set  $S_3A$  and MTA exhibited attachment of MDPs on their surface.  $S_3A$  extract showed significantly higher mineralized nodule formation and mRNA expression of Bmp2, Oc, and Opn than did MTA extract. SBF-dipped  $S_3A$  exhibited formation of surface precipitates, which were composed of Ca, P, Sr, and Al. Direct pulp capping with  $S_3A$  and with MTA induced mineralized tissue repair of the exposed pulp.

\* Corresponding author. Department of Pulp Biology and Endodontics, Division of Oral Health Sciences, Graduate School of Medical and Dental Sciences, Tokyo Medical and Dental University (TMDU), 1-5-45 Yushima, Bunkyo-ku, Tokyo, 113-8549, Japan.

E-mail address: [k.hashimoto.endo@tmd.ac.jp](mailto:k.hashimoto.endo@tmd.ac.jp) (K. Hashimoto).

**Conclusion:** S<sub>3</sub>A possesses biocompatibility and pro-mineralization effects comparable to those of MTA.

© 2022 Association for Dental Sciences of the Republic of China. Publishing services by Elsevier B.V. This is an open access article under the CC BY-NC-ND license (<http://creativecommons.org/licenses/by-nc-nd/4.0/>).

## Introduction

Mineral trioxide aggregate (MTA) is a Portland cement-derived hydraulic material that shows favorable clinical outcomes in several endodontic applications, including direct pulp capping<sup>1</sup> and root-end filling.<sup>2</sup> This is largely because MTA has low cytotoxicity<sup>3,4</sup> and marked capacity for inducing mineralized tissue formation in the exposed dental pulp.<sup>5–8</sup> MTA mainly consists of tricalcium silicate (3CaO·SiO<sub>2</sub>; C<sub>3</sub>S), and its bioactivity is related to its capacity to release calcium (Ca) and hydroxyl ions, producing apatite-like precipitates.<sup>9</sup> However, bismuth oxide added to MTA as a radiopacifying agent<sup>10–12</sup> causes adverse effects to MTA, including an extension in setting time, a decrease in compressive strength,<sup>10</sup> and tooth discoloration.<sup>11,12</sup> Some reports have raised concerns about the toxicity of bismuth oxide.<sup>13,14</sup>

In a previous study,<sup>15</sup> tristrontium aluminate (3SrO·Al<sub>2</sub>O<sub>3</sub>; S<sub>3</sub>A), which is a hydraulic cement with hydration and setting behaviors similar to those of MTA,<sup>16</sup> was prepared. Evaluation of the physical properties of S<sub>3</sub>A showed higher flowability and a shorter setting time than MTA. Additionally, the radiopacity of S<sub>3</sub>A was similar to that of MTA.<sup>15</sup>

There has been increased interest in strontium (Sr)-based bioactive cements as a new alternative to MTA. Sr is an alkaline earth element similar to Ca, and Sr ions can be incorporated into tooth hydroxyapatite, improving acid resistance and promoting remineralization.<sup>17–20</sup> Strontium ranelate is a commercially available drug for osteoporosis treatment, which promotes osteoblastic bone formation and inhibits resorption by osteoclasts.<sup>21</sup> Strontium ranelate is shown to induce mineralized tissue repair in exposed rat dental pulp and to promote proliferation and differentiation of mouse dental papilla cells (MDPs).<sup>22</sup> Moreover, the addition of strontium ranelate significantly improves the radiopacity and osteogenesis of calcium phosphate cement.<sup>23</sup>

S<sub>3</sub>A would be a promising candidate as an alternative to MTA if its biological effects are shown to be similar to or better than MTA. Thus, the aim of this study was to

investigate the biocompatibility and pro-mineralization effects of S<sub>3</sub>A in comparison with a commercially available MTA (ProRoot MTA White; Dentsply Sirona, Ballaigues, Switzerland).

## Materials and methods

### Cement preparation

S<sub>3</sub>A was prepared as previously described.<sup>15</sup> Strontium hydroxide octahydrate (Kanto Chemical, Tokyo, Japan) and aluminum hydroxide (Kanto Chemical) powders were mixed at 3:2 M ratio, calcined at 1200 °C and ground to obtain S<sub>3</sub>A powder.

### Preparation of S<sub>3</sub>A and MTA extracts and quantification of elemental concentrations

S<sub>3</sub>A was mixed with water at a water/powder ratio of 0.6 and placed in a 3D-printed round mold with internal dimensions of 1 mm thickness and 8 mm diameter. MTA was mixed according to the manufacturer's instructions. Both cements were incubated for 24 h at 37 °C and 100% relative humidity until final setting.

Ion dissolution from S<sub>3</sub>A extract solution was estimated by immersion in 10 mL of ultrapure water in a sealed container at 37 °C for 1, 3, and 7 d. The resulting solutions were centrifuged and filtered with a syringe filter (0.2 μm in pore diameter, Advanced Microdevices, Ambala Cantt, India). The ion concentration in the extract solutions was determined by inductively coupled plasma atomic emission spectroscopy (ICP-AES; Spectro Arcos, Hitachi High-Technologies, Tokyo, Japan). A multi-element standard solution (10 ppm, XSTC-622, Seishin Trading, Kobe, Japan) was used as the standard. Based on the time-course change of ion concentration, 3-day extract solutions for S<sub>3</sub>A and MTA were applied for the following experiments after sterilization with the syringe filter (see Table 1).

### Cell culture

MDPs were obtained from the incisor apical buds of mice and then immortalized by transfection with human papilloma virus.<sup>24</sup> Alpha-modified minimum essential medium (α-MEM; Wako Pure Chemical, Osaka, Japan) was used for culturing, after addition of 10% fetal bovine serum (FBS; GE Healthcare, Chicago, IL, USA) and 1% antibiotic and antifungal solution (Penicillin-Streptomycin-Amphotericin B Suspension, Wako Pure Chemical). Cultures were maintained at 37 °C, 5% CO<sub>2</sub>, and 100% humidity, and the medium was changed every 3 d.

**Table 1** Ion concentration analysis for S<sub>3</sub>A cement in ultrapure water for 1, 3 and 7 d.

	Immersion period (d)		
	1	3	7
Sr (mol/dm)	0.07 (0.03)	11.0 (0.72)	16.2 (1.79)
Al (mol/dm)	2.32 (1.24)	18.6 (0.72)	24.1 (1.44)

Mean (SD), n = 4.

S<sub>3</sub>A and MTA extract solutions were diluted with  $\alpha$ -MEM at 1/8 concentration (1/8-S<sub>3</sub>A and 1/8-MTA, respectively).  $\alpha$ -MEM was used as a negative control, after adding ultra-pure water at 1/8 concentration.

### Cell proliferation assay

MDPs ( $3 \times 10^3$  cells/well) were seeded in a 96-well plate. After 24 h, the media were changed to 1/8-S<sub>3</sub>A, 1/8-MTA and  $\alpha$ -MEM (control). Cell proliferation was measured at 1, 2, and 3 d using a tetrazolium-salt assay (Cell Counting Kit-8, Dojindo Laboratories, Kumamoto, Japan).

### Cell attachment

S<sub>3</sub>A and MTA were mixed under aseptic conditions, placed into 3D-printed round molds, and incubated for 24 h. The molds were then inserted in a 24-well plate, and MDPs ( $1 \times 10^5$  cells/well) were seeded over the cement surface and cultured for 3 d.

Samples ( $n = 3$  for each group) were fixed in 2.5% glutaraldehyde (Wako Pure Chemical) for 2 h, post-fixed with 1% OsO<sub>4</sub> (TAAB, Aldermaston, UK), and dehydrated in a critical point drying apparatus (HCP-2; Hitachi, Tokyo, Japan). The samples were then carbon-coated with platinum (E102, Hitachi) and examined under a scanning electron microscope (SEM; S-3400NX, Hitachi High-Tech).

### Mineralized nodule formation

MDPs ( $1 \times 10^4$  cells/well) were seeded in a 48-well plate, and cultured for 48 h. The media were then changed to 1/8-S<sub>3</sub>A, 1/8-MTA, and  $\alpha$ -MEM (control). All cultures were supplemented with L-ascorbic acid (0.2 mM; Wako Pure Chemical) and  $\beta$ -glycerophosphate (5.0 mM; Sigma Aldrich, St. Louis, MO, USA). The resulting mineralized nodules were stained using Alizarin Red S (Wako Pure Chemical) at 4 d and the stained area was measured using ImageJ software (<https://imagej.net/ImageJ2>).

### Odonto/osteogenic marker gene expression

MDPs ( $5 \times 10^4$  cells/well) were cultured for 24 h in a 12-well plate. The media were then changed to 1/8-S<sub>3</sub>A, 1/8-MTA, and  $\alpha$ -MEM (control). After 3 d, total RNA was extracted using an ultra-thin polymer membrane (QuickGene, Kurabo, Osaka, Japan) and cDNA was synthesized (PrimeScript RT Reagent Kit: Perfect Real Time, Takara, Shiga, Japan). The reverse transcription-quantitative polymerase chain reaction (RT-qPCR) assay was performed with the CFX96 Real-Time PCR Detection System (Bio-Rad, Hercules, CA, USA) using primers for bone morphogenic protein (Bmp2), osteocalcin (Oc), osteopontin (Opn), and beta-actin (Ba) as internal controls. The primer sequences are presented in Table 2.

### Elemental analysis of surface precipitates using energy dispersive X-ray analysis

S<sub>3</sub>A was mixed, placed into 3D-printed molds, and incubated for 24 h. Simulated body fluid (SBF) was prepared

according to the methods of Kokubo and Takadama.<sup>25</sup> The set cement samples were immersed in SBF and kept in an incubator for 28 d. Non-immersed samples served as controls. Then, all specimens were dried at the critical point, carbon-coated (EC-32010CC, JEOL, Tokyo, Japan), and examined with SEM (JSM-7900F, JEOL) and energy dispersive X-ray analysis (EDX) (JED-2300, JEOL) under acceleration voltage of 15 keV.

### Direct pulp capping *in vivo* and histological examination

All animal experiments were approved by the Institutional Animal Care and Use Committee (A2021-251A), and all experimental procedures were performed in accordance with National Research Council's Guide for the Care and use of Laboratory Animals. Wistar rats ( $n = 6$ , male, 5-weeks old, Clea Japan, Tokyo, Japan) were anesthetized with intraperitoneal injection of ketamine hydrochloride (90 mg/kg; Ketalar; Sankyo, Tokyo, Japan) and xylazine hydrochloride (10 mg/kg; Selactar; Bayer Yakuin, Osaka, Japan). Cavities were prepared in the occlusal surface of the upper first and second molars with a #1/2 round bur (Meisinger ST1 HP 005; Kulzer, Hanau, Germany) using a dental handpiece motor (J Morita, Osaka, Japan) under a dental microscope (Dental Microscope Z; Mani, Tochigi, Japan). After pulp exposure was confirmed in the cavities, bleeding was controlled using sterile cotton pellets. S<sub>3</sub>A and MTA were mixed as described above and applied over the exposed pulp at a thickness of approximately 0.15 mm, using an MTA carrier (Dentech, Tokyo, Japan). In the control group, neither S<sub>3</sub>A nor MTA was applied. The cavities were sealed with a resin-modified glass ionomer cement (Ionosit-Baseliner; DMG, Hamburg, Germany).

After 2 and 4 weeks, the rats were sacrificed by CO<sub>2</sub> euthanasia. The upper jaws were dissected and fixed with 4% paraformaldehyde for 24 h at 4 °C. Samples were demineralized with 17% EDTA for 3 weeks, embedded in an embedding medium (OCT compound, Sakura Finetek, Torrance, CA, USA), and frozen in liquid nitrogen. Sagittal sections 10  $\mu$ m thick were cut in a cryostat (CM3050; Leica, Wetzlar, Germany), and stained with hematoxylin and eosin. The number of specimens were 3 teeth per group for each period.

### Statistical analysis

Data were analyzed using statistical software (Prism 6, GraphPad, San Diego, CA, USA). One-way analysis of variance followed by a Tukey *post hoc* test was used for multiple comparisons. A P-value of <0.05 was considered statistically significant.

## Results

### Concentration of Sr and Al released from S<sub>3</sub>A

As shown in Table 1, the concentration of Sr and Al increased up to 3 d and increased slightly thereafter up to 7 d. Because the concentrations were near saturation, the

**Table 2** Primer sequences.

Gene	Forward Primer	Reverse Primer
Target	(5'–3')	(5'–3')
Bmp2	ACACAGCATGCCTTAGGGATT	AGACACCCTTTGTATGTGGACT
Oc	CATACTGGTCTGATAGCTCGTCAC	AGGGCAATAAGGTAGTGAACAGAC
Opn	TTCGGAATTTTCAGATACCTATCATC	GATGTGATCGATAGTCAAGCAAGTT
Ba	GTAAGACCTCTATGCCAACACAGT	AATGATCTTGATCTTCATGGTGCTA

Bmp2: bone morphogenic protein 2, Oc: osteocalcin, Opn: osteopontin, Ba: beta-actin.

3-d-immersed solution was applied to the following *in vitro* analysis. MTA extract solution was prepared with 3-d immersion to match the preparation method of the S<sub>3</sub>A extract solution.

### MDP proliferation

As shown in Fig. 1A, there were no significant differences between the three groups at 1 d. At 2 d, 1/8-MTA exhibited

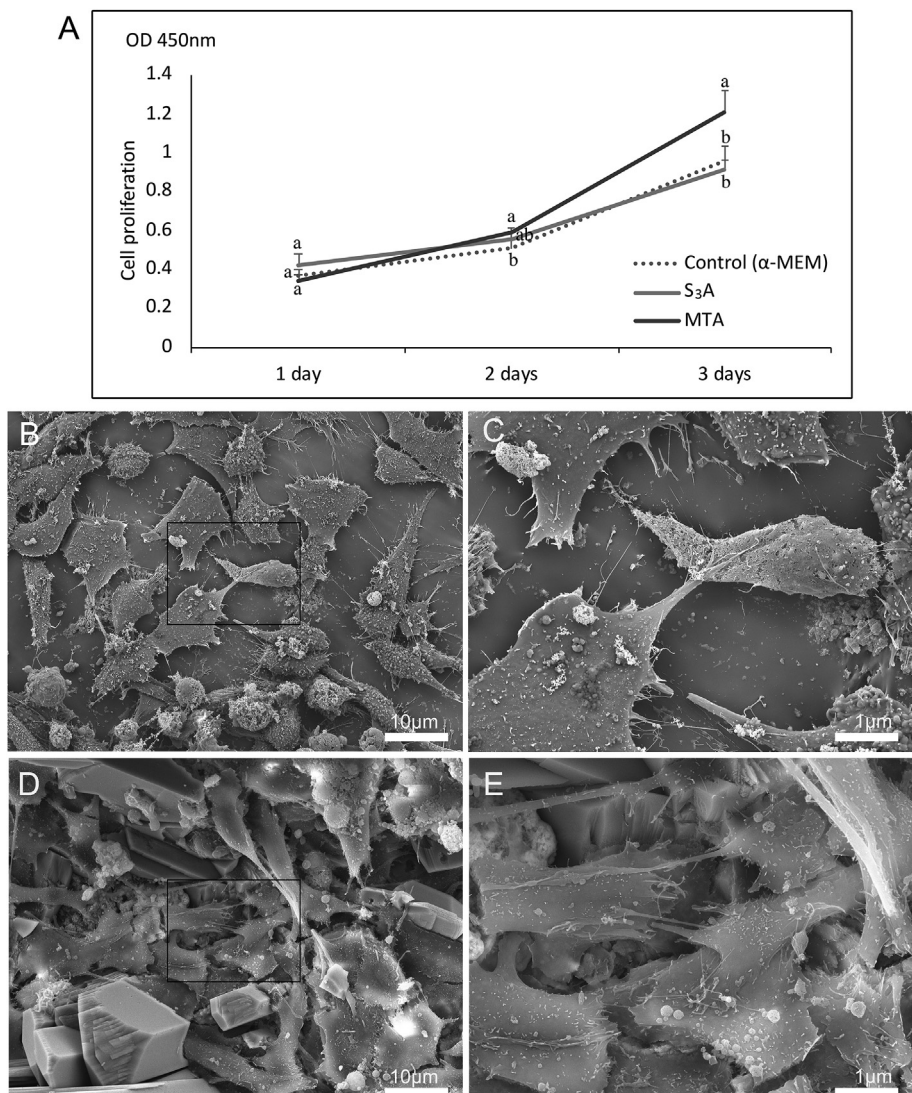


**Figure 1** (A) The effect of 1/8 dilutions of S<sub>3</sub>A and mineral trioxide aggregate (MTA) extract solutions and control (alpha-modified minimum essential medium [α-MEM]) on the proliferation of mouse dental papilla cells (MDPs) at 1, 2, and 3 d. Different letters at the same time point indicate significant differences. \*P < 0.05, n = 4. (B–E) Representative scanning electron microscope photomicrographs showing the ultrastructure of MDPs attached on set S<sub>3</sub>A (B, C) and MTA (D, E). C and E are high-power views (× 3K magnification) of the boxed areas indicated in B and C (× 1K magnification), respectively.

significantly higher cell proliferation than the control ( $P < 0.05$ ), but was not significantly higher in comparison to 1/8- $S_3A$ . At 3 d, there was no significant difference between 1/8- $S_3A$  and the control, but 1/8-MTA showed a significantly higher value in comparison to both ( $P < 0.05$ ).

### Cell attachment

SEM observation showed MDPs with a spindle shape with extended cytoplasmic processes attached on the surface of  $S_3A$  (Fig. 1B and C) and MTA (Fig. 1D and E). The cell morphology and distribution were similar between the two groups.

### Mineralized nodule formation

As shown in Fig. 2A and B, MDPs cultured with  $S_3A$  extract for 4 d exhibited a significantly larger stained area compared with those cultured with MTA and the control ( $P < 0.05$ ).

### Odonto/osteogenic marker gene expression

MDPs cultured with  $S_3A$  extract solution recorded significantly higher mRNA expression of *Bmp2*, *Op*, and *Oc* in

comparison to MDPs cultured with MTA and the control ( $P < 0.05$ ; Fig. 2C).

### Surface precipitate formation after immersion in SBF

After immersion in SBF for 28 d, formation of precipitates was observed over the  $S_3A$  samples (Fig. 3C). Elements detected in non-immersed  $S_3A$  samples were aluminum (Al) and Sr, which are the components of  $S_3A$  (Fig. 3B). In contrast, the specimen surface after SBF-immersion showed Ca and P peaks, which would be derived from calcium phosphate precipitates on the cement surface (Fig. 3D).

### Mineralized tissue repair of exposed pulps capped with $S_3A$

As shown in Fig. 4,  $S_3A$  and MTA directly applied to mechanically exposed rat molar pulp similarly induced the formation of mineralized tissue with an atubular, osteodentin-like structure. At 2 weeks, a thin layer of newly formed mineralized tissue was seen along the exposure site, while a thick mass of newly formed mineralized tissue was observed at 4 weeks. In the control group, no

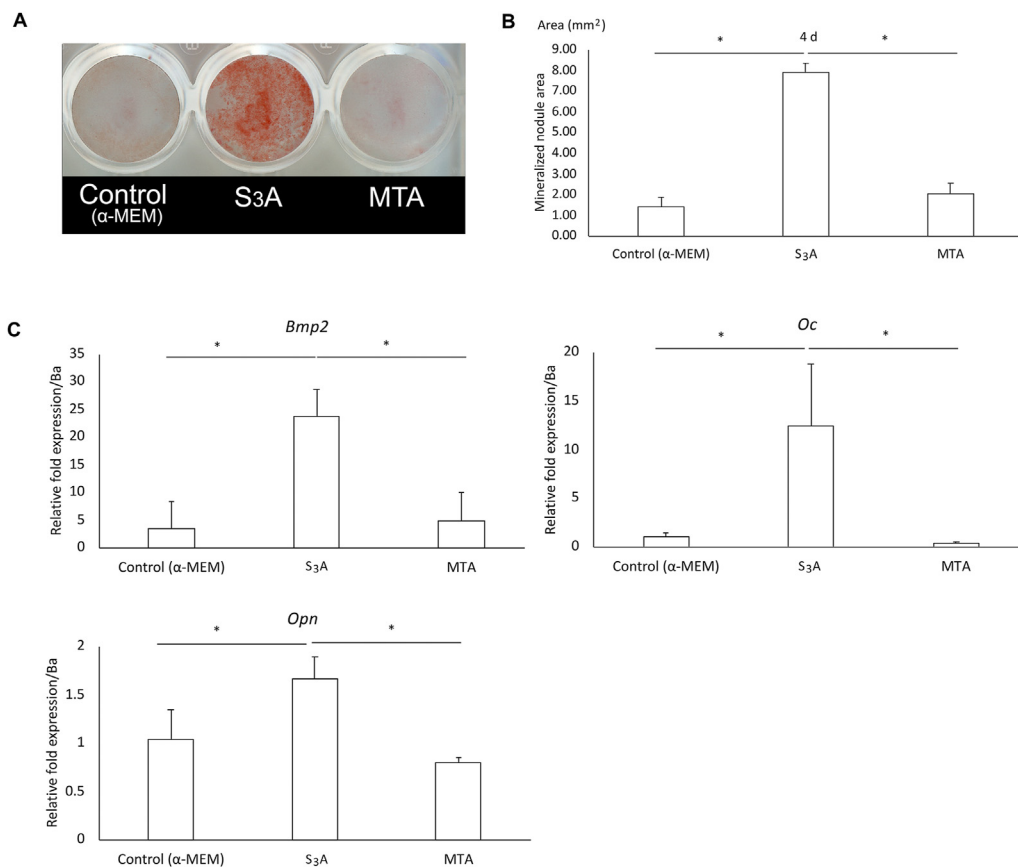


**Figure 2** (A, B) Mineralized nodule formation in mouse dental papilla cells (MDPs) cultured with  $S_3A$ , mineral trioxide aggregate (MTA) and control (alpha-modified minimum essential medium [ $\alpha$ -MEM]) in osteogenic conditions. (A) Representative images. (B) Mineralized nodule area (mean and SD,  $n = 3$ ). (C) Expression of mRNAs for bone morphogenic protein (*Bmp2*), osteocalcin (*Oc*) and osteopontin (*Opn*) in MDPs cultured with  $S_3A$ , MTA and control (mean and SD,  $n = 3$ ). \* $P < 0.05$ .

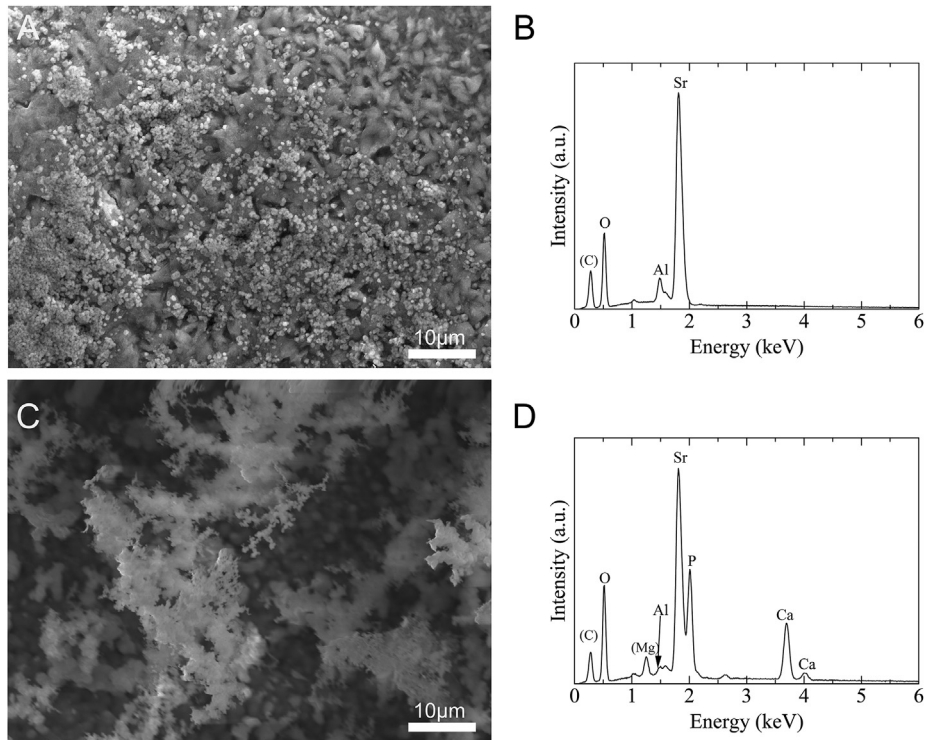


**Figure 3** Scanning electron microscope images (A, C) and energy dispersive X-ray analysis (EDX) spectra (B, D) of set  $S_3A$  cement not immersed in simulated body fluid (SBF) (A, B), and immersed in SBF for 28 d (C, D).

mineralized tissue formation was observed at the pulp exposure site.

## Discussion

The drawbacks of MTA, particularly its bismuth oxide content, has led to an interest in the development of new endodontic cements that provide sufficient inherent radiopacity, high biocompatibility, and pro-mineralization ability.  $S_3A$  was chosen because it exhibits hydration and setting mechanisms similar to MTA cements,<sup>16</sup> and has a shorter setting time, higher flowability, and similar radiopacity in comparison to MTA.<sup>15</sup> The present study evaluated the biological effects of  $S_3A$  in terms of biocompatibility and its ability to promote odonto/osteogenic differentiation and mineralization. MDPs were chosen as pulp-like cells with the potential for odonto/osteogenic differentiation.

The proliferation of MDPs was not inhibited by 1/8- $S_3A$  at 1–3 d in comparison to the control. The proliferation of MDPs with 1/8-MTA was similar to that of MDPs with 1/8- $S_3A$  at 1 and 2 d, but was significantly higher at 3 d. A previous report has shown that strontium ranelate causes up-regulation of MDP proliferation.<sup>22</sup> Another study demonstrated that Sr promoted the proliferation of human dental pulp stem cells in a dose-dependent manner.<sup>26</sup> The present results did not show a similar promoting ability of  $S_3A$ , but indicated that  $S_3A$  does not disturb the proliferation of MDPs. The lack of promotion of MDP cell proliferation by  $S_3A$  could be explained by the different methodology of cement extract preparation or different dilution ratios in previous studies.

Cell adhesion is mandatory for subsequent cell growth, cytodifferentiation, and extracellular matrix production. Moreover, cells in contact with a biomaterial can be directly affected if the material releases toxic components. Thus, the assessment of cell attachment onto biomaterials is considered fundamental when evaluating the cytocompatibility of biomaterials.<sup>27</sup> MDPs were shown to fully grow and attach over the surface of set  $S_3A$  and MTA (Fig. 1B–E), which is in accordance with previous studies showing the favorable attachment properties of MTA.<sup>27</sup> MDPs exhibited similar morphology and distribution between the two cements, which is considered a positive indication for the biocompatibility of  $S_3A$ .

In the present study,  $S_3A$  significantly increased the mRNA expression of Bmp2, Oc, and Opn compared with MTA and control groups. This is consistent with the previous finding that strontium ranelate promotes osteo/odonto-genic gene expression of MDPs.<sup>22</sup> Bmp2 was chosen for its role in the regulation of odontoblastic differentiation and dentin formation.<sup>28</sup> Oc was chosen because it is a representative late stage marker gene for odontoblastic differentiation and plays a role in the formation of mineralized matrix.<sup>29</sup> Opn was chosen because it plays a key role in the differentiation of odontoblast-like cells during dentin repair.<sup>6</sup> Moreover,  $S_3A$  extract solution significantly increased mineralized nodule formation in MDPs, which is in accordance with the increase in mineralized nodule formation by strontium ranelate in MDPs,<sup>22</sup> and by Sr in human dental pulp cells.<sup>26</sup> The present findings indicate that  $S_3A$  possesses the ability to promote mineralized tissue formation, supporting the notion that  $S_3A$  is a useful alternative

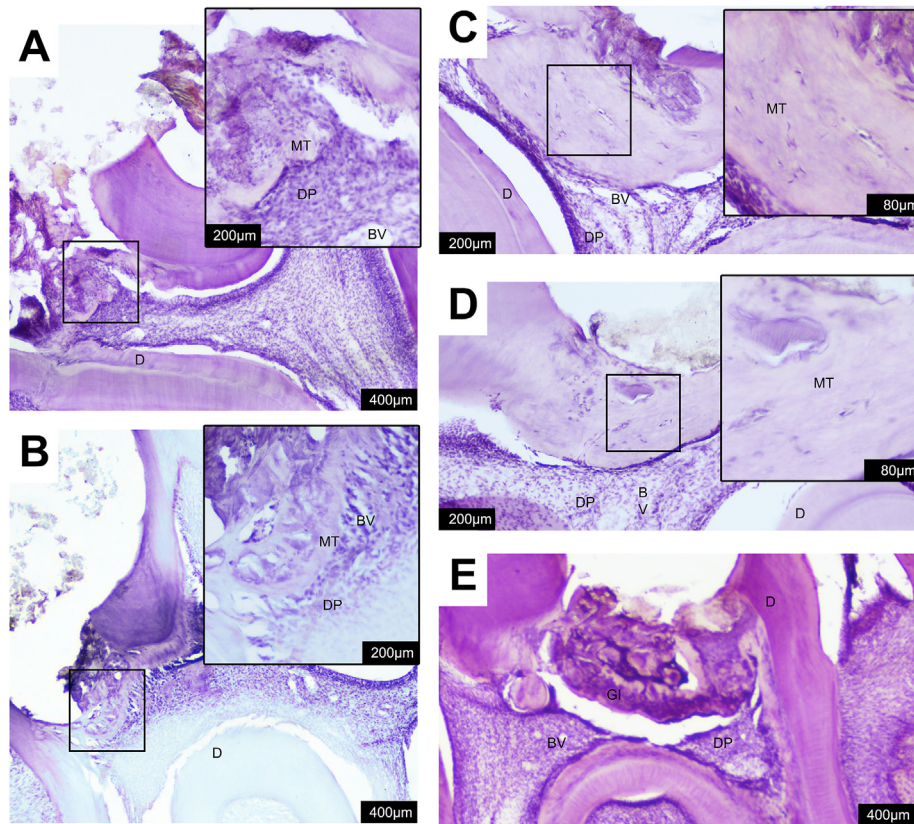


**Figure 4** Representative images of rat molars after pulp capping with  $S_3A$  (A, C) or mineral trioxide aggregate (MTA) (B, D). (E) Control with no pulp capping material. Specimens were obtained at 2 weeks (A, B, E) and 4 weeks (C, D). Hematoxylin and eosin staining. Insets are higher magnification views of the boxed areas. D: dentin, DP: dental pulp, MT: newly formed mineralized tissue, GI: glass ionomer cement, BV: blood vessel.

to MTA. Such properties of  $S_3A$  can be attributed to the release of Sr, which is known to stimulate the differentiation of osteoblasts<sup>30</sup> and odontoblasts<sup>31</sup> through mechanisms involving the calcium-sensing receptor.

Apatite formation on the surface of a material in SBF is a popular method by which *in vivo* material-mineralized tissue connection can be predicted,<sup>25</sup> and this property is considered as a basis for the bioactivity of several inorganic biomaterials,<sup>32</sup> including MTA.<sup>9</sup> This study demonstrated that  $S_3A$  produced surface precipitates containing Ca and P, indicating the formation of calcium phosphate phases. The precipitates also contained Sr, which could be incorporated in the calcium phosphate phases as the substitute for Ca.<sup>17,20</sup> The precipitate formation on the surface of SBF-exposed  $S_3A$  indicates *in vitro* bioactivity essential for mineralized tissue-inductive biomaterials.

*In vivo* application of  $S_3A$  and MTA to rat exposed pulps induced the deposition of mineralized tissue occluding the pulp exposure site. The mineralized tissue showed an osteodentin-like morphology, with an atubular appearance and sparse cellular inclusions. This was in line with the finding that osteodentin-like mineralized tissue was formed in rat pulp topically applied with strontium ranelate.<sup>22</sup> Although formation of tissues with a tubular dentin-like structure could be more desirable, the dense and almost acellular structure of the osteodentin-like tissue suggests it is impermeable enough to protect

the underlying pulp tissue from exogenous noxious substances. The present findings may support the notion that  $S_3A$  can be substituted for MTA as a pulp-capping agent with a capacity to induce mineralized tissue repair of the exposed pulp.

In conclusion, within the limitations of this study,  $S_3A$  possessed biocompatibility and pro-mineralization effects comparable to those of MTA. These findings suggest that  $S_3A$  is a viable candidate for an endodontic biomaterial capable of promoting mineralized tissue formation, and that  $S_3A$  can be used as an alternative to MTA, or as a radiopacifying agent for MTA. Future studies are required to explore the mechanisms by which  $S_3A$  promotes mineralized tissue formation.

### Declaration of competing interest

The authors declare no conflicts of interest.

### Acknowledgments

This work was supported by a Grant-in Aid for Scientific Research from the Japan Society for the Promotion of Science (JSPS; No.20H03869). We thank Helen Jeays, BDSc AE, from Edanz (<https://jp.edanz.com/ac>) for editing a draft of this manuscript.

## References

1. Kundzina R, Stangvaltaite L, Eriksen HM, Kerosuo E. Capping carious exposures in adults: a randomized controlled trial investigating mineral trioxide aggregate versus calcium hydroxide. *Int Endod J* 2017;50:924–32.
2. Safi C, Kohli MR, Kratchman SI, Setzer FC, Karabucak B. Outcome of endodontic microsurgery using mineral trioxide aggregate or root repair material as root-end filling material: a randomized controlled trial with cone-beam computed tomographic evaluation. *J Endod* 2019;45:831–9.
3. Kettering JD, Torabinejad M. Investigation of mutagenicity of mineral trioxide aggregate and other commonly used root-end filling materials. *J Endod* 1995;21:537–9.
4. Sumer M, Muglali M, Bodrumlu E, Guvenc T. Reactions of connective tissue to amalgam, intermediate restorative material, mineral trioxide aggregate, and mineral trioxide aggregate mixed with chlorhexidine. *J Endod* 2006;32:1094–6.
5. Accorinte Mde L, Holland R, Reis A, et al. Evaluation of mineral trioxide aggregate and calcium hydroxide cement as pulp-capping agents in human teeth. *J Endod* 2008;34:1–6.
6. Kuratate M, Yoshida K, Shigetani Y, Yoshida N, Ohshima H, Okiji T. Immunohistochemical analysis of nestin, osteopontin, and proliferating cells in the reparative process of exposed dental pulp capped with mineral trioxide aggregate. *J Endod* 2008;34:970–4.
7. Faraco Jr IM, Holland R. Response of the pulp of dogs to capping with mineral trioxide aggregate or a calcium hydroxide cement. *Dent Traumatol* 2001;17:163–6.
8. Didilescu AC, Cristache CM, Andrei M, Voicu G, Perlea P. The effect of dental pulp-capping materials on hard-tissue barrier formation: a systematic review and meta-analysis. *J Am Dent Assoc* 2018;149:903–17.
9. Gandolfi MG, Taddei P, Tinti A, Prati C. Apatite-forming ability (bioactivity) of ProRoot MTA. *Int Endod J* 2010;43:917–29.
10. Antonijevec D, Medigovic I, Zrilic M, Jokic B, Vukovic Z, Todorovic L. The influence of different radiopacifying agents on the radiopacity, compressive strength, setting time, and porosity of Portland cement. *Clin Oral Invest* 2014;18:1597–604.
11. Marciano MA, Costa RM, Camilleri J, Mondelli RF, Guimarães BM, Duarte MA. Assessment of color stability of white mineral trioxide aggregate angelus and bismuth oxide in contact with tooth structure. *J Endod* 2014;40:1235–40.
12. Marciano M, Duarte M, Camilleri J. Dental discoloration caused by bismuth oxide in MTA in the presence of sodium hypochlorite. *Clin Oral Invest* 2015;19:2201–9.
13. Thomas F, Bialek B, Hensel R. Medical use of bismuth: the two sides of the coin. *J Clin Toxicol* 2011;3:4.
14. Abudayyak M, Öztaş E, Arici M, Özhan G. Investigation of the toxicity of bismuth oxide nanoparticles in various cell lines. *Chemosphere* 2017;169:117–23.
15. Adel S, Wada T, Kawashima N, et al. Preparation and properties of tristrontium aluminate as an alternative component of mineral trioxide aggregate (MTA) cement. *Dent Mater J* 2021;40:184–90.
16. Ptáček P, Šoukal F, Opravil T, Bartoničková E, Zmrzlý M, Novotný R. Synthesis, hydration and thermal stability of hydrates in strontium-aluminate cement. *Ceram Int* 2014;40:9971–9.
17. Dedhiya MG, Young F, Higuchi WI. Mechanism for the retardation of the acid dissolution rate of hydroxyapatite by strontium. *J Dent Res* 1973;52:1097–109.
18. Featherstone JDB, Shields CP, Khademazad B, Oldershaw MD. Acid reactivity of carbonated apatites with strontium and fluoride substitutions. *J Dent Res* 1983;62:1049–53.
19. Thuy TT, Nakagaki H, Kato K, et al. Effect of strontium in combination with fluoride on enamel remineralisation in vitro. *Arch Oral Biol* 2008;53:1017–22.
20. Uo M, Wada T, Asakura K. Structural analysis of strontium in human teeth treated with surface pre-reacted glass-ionomer filler eluate by using extended X-ray absorption fine structure analysis. *Dent Mater J* 2017;36:214–21.
21. Rossi AL, Moldovan S, Querido W, et al. Effect of strontium ranelate on bone mineral: analysis of nanoscale compositional changes. *Micron* 2014;56:29–36.
22. Bakhit A, Kawashima N, Hashimoto K, et al. Strontium ranelate promotes odonto-/osteogenic differentiation/mineralization of dental papillae cells in vitro and mineralized tissue formation of the dental pulp in vivo. *Sci Rep* 2018;8:9224.
23. Wu T, Yang S, Lu T, et al. Strontium ranelate simultaneously improves the radiopacity and osteogenesis of calcium phosphate cement. *Biomed Mater* 2019;14. 35005–035005.
24. Tsubakimoto T, Kousaka K, Saito M, et al. Immortalization of dental papilla cells differentiating into odontoblast in vitro. *J Conserv Dent* 2007;50:292–301.
25. Kokubo T, Takadama H. How useful is SBF in predicting in vivo bone activity? *Biomaterials* 2006;27:2907–25.
26. Huang M, Hill RG, Rawlinson SCF. Strontium (Sr) elicits odontogenic differentiation of human dental pulp stem cells (hDPSCs): a therapeutic role for Sr in dentine repair? *Acta Biomater* 2016;38:201–11.
27. Ahmed HMA, Luddin N, Kannan TP, Mokhtar KI, Ahmed A. Cell attachment properties of Portland cement-based endodontic materials: biological and methodological considerations. *J Endod* 2014;40:1517–23.
28. Yang J, Ye L, Hui TQ, et al. Bone morphogenetic protein 2-induced human dental pulp cell differentiation involves p38 mitogen-activated protein kinase-activated canonical WNT pathway. *Int J Oral Sci* 2015;7:95–102.
29. Tani-Ishii N, Hamada N, Watanabe K, Tujimoto Y, Teranaka T, Umemoto T. Expression of bone extracellular matrix proteins on osteoblast cells in the presence of mineral trioxide. *J Endod* 2007;33:836–9.
30. Marx D, Yazdi AR, Papini M, Towler M. A review of the latest insights into the mechanism of action of strontium in bone. *BoneKEy Rep* 2020;12:100273.
31. Mizumachi H, Yoshida S, Tomokiyo A, et al. Calcium-sensing receptor-ERK signaling promotes odontoblastic differentiation of human dental pulp cells. *Bone* 2017;101:191–201.
32. Kasuga T. Bioactive calcium pyrophosphate glasses and glass-ceramics. *Acta Biomater* 2005;1:55–64.